///VSP/// *Journal of Adhesion Science and Technology 25 (2011) 581–596*

Journal of ADHESION SCIENCE and TECHNOLOGY
brill.nl/jast

Effect of Inorganic Fillers in Paper on the Adhesion of Pressure-Sensitive Adhesives

Weixu Chen [a], **Xiaoyan Tang** [a], **John Considine** [b] **and Kevin T. Turner** [a]*

[a] Department of Mechanical Engineering, University of Wisconsin, Madison, WI 53706, USA
[b] US Forest Service, Forest Products Laboratory, Madison, WI 53726, USA

Abstract
Inorganic fillers are inexpensive materials used to increase the density, smoothness and other properties of paper that are important for printing. In the current study, the adhesion of pressure-sensitive adhesives (PSAs), a common type of adhesive used in labels and tapes, to papers containing varying amounts and types of fillers is investigated. Papers with three types of fillers, precipitated calcium carbonate (PCC), ground calcium carbonate (GCC) and kaolin clay, were investigated. The compositions of the papers were examined with SEM/EDX, while peel and double cantilever beam (DCB) tests were used to assess PSA–paper adhesion. The results indicate that fillers enhance the adhesion between PSA and paper. In the case of the peel tests, a combination of inter-fiber bond strength and PSA–paper adhesion determines the peel strength. While in the DCB tests, failure is isolated to the PS A-paper interface, thus allowing measurements of pure interfacial failure.
© Koninklijke Brill NV, Leiden, 2011

Keywords
Pressure sensitive adhesive, double cantilever beam, fillers

1. Introduction

Inorganic fillers or mineral fillers, such as clay, calcite, aragonite and talc, are inexpensive materials that are frequently incorporated in paper to improve its properties and reduce cost. Most copy papers made in North America contain more than 10 weight percent of kaolin clay. In modern papermaking, the primary use of these fillers is to improve printing and optical properties, such as density, opacity, brightness and smoothness.

Three types of commercial fillers were used in the present study: kaolin clay, precipitated calcium carbonate (PCC) and ground calcium carbonate (GCC). Kaolin is a natural clay composed of fine grain, well-crystallized, hexagonal particles. Calcium carbonates are naturally occurring or can be precipitated from limestone

*To whom correspondence should be addressed. Tel.: 608-890-0913; e-mail: kturner@engr.wisc.edu

© Koninklijke Brill NV, Leiden, 2011 DOI:10.1163/016942410X525830

or other chemical reactions. The geometry of calcium carbonate filler particles is strongly influenced by the production method. PCCs from calcite and argonite have trigonal–rhombohedral, trigonal–scalenohedral and orthorhombic shapes. GCCs have irregular geometries that result from the mechanical grinding processes used to make them. For all three inorganic filler types, the size can vary from nanometers to micrometers [1].

As fillers are routinely used in the manufacture of paper, the effects of fillers on paper properties have been widely investigated. Some issues associated with the use of fillers include retention, aggregation, *z*-profile distribution, inter-fiber bonding disruption, drainage, chemical reactivity, and increased friction-induced wear. Filler particles are not easily retained in the sheet without the addition of polymeric retention aids, because they are small compared to pulp fibers and because both fillers and pulp fibers are negatively charged. Depending on pulp furnish, addition of filler particles may impact paper strength and rigidity as their presence disrupts fiber–fiberbonding [2, 3]. The interactions of fillers and cellulose fibers have been well-documented, but the influence of fillers on adhesion of pressure-sensitive adhesive (PSAs) to papers containing inorganic surface particles has not received similar attention. The effect of fillers in paper on PSA–paper adhesion strength is the focus the present work.

Motivation for this work is provided by the influx of PSA products designed to adhere to paper in the consumer marketplace. PSAs are the adhesive of choice for most labels, sticky notes and postage stamps. Current evaluation of PSA behavior is accomplished by techniques such as tack, peel and rolling ball that were designed for other applications [4]. Previous works on PSA–paper adhesion such as that by Zhao and coworkers [5–7]and Pelton *et al.* [8] illustrate the complexities of characterizing PSA–paper adhesion and that the paper properties, such as internal bond strength, often influence the measured adhesion strength. While these previous studies have contributed greatly to our understanding of PSA–paper adhesion, none of them directly examines the role of fillers in determining PSA–paper adhesion strength.

This work presents results of a systematic experimental study to characterize the effects of inorganic fillers on PSA–cellulose interfacial properties.

2. Materials and Methods

2.1. Pressure-Sensitive Adhesive

In all experiments, the PSA and carrier material were a repositionable coated-paper label from a commercial supplier (Avery, product #55160). During PSA application, the coating package is continually modified, based on factory environmental conditions, to produce a uniform and repeatable product. A commercial product was selected for this work because industrial production greatly reduces common laboratory sample preparation problems, such as non-uniform thickness and incomplete coverage. In the current work, the PSA label was always adhered to the top

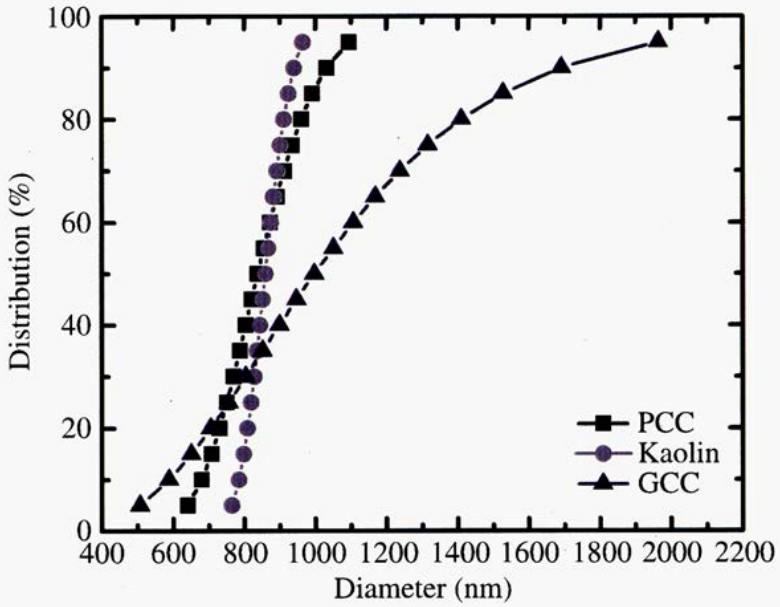

Figure 1. Particle size distribution for each type of filler.

surface of a handsheet, which is the surface opposite of the forming wire during paper production.

2.2. Fillers

Three kinds of fillers: (1) rhombic PCC (Mississippi Lime, St. Genevieve, MO), (2) hexagonal kaolin clay (Imerys, Roswell, GA) and (3) GCC (Imerys) were used in the current work. Figure 1 summarizes size distributions of the filler particles. These distributions were measured using a laser scattering particle analyzer (model LA-910, Brookhaven Instruments Corporation, Long Island, NY).

2.3. Handsheet Preparation

Pulp furnish consisted of a 100% bleached hardwood eucalyptus kraft pulp beaten to 450 ml CSF (Canadian Standard Freeness) at pH 7.0. Before sheet making, the beaten pulp was color treated using Rit® Black15 liquid dye in order to facilitate identification of paper failure in the DCB (double cantilever beam) and peel tests. Handsheets were produced to a target basis weight of 60 g/m^2 as per TAPPI Standard T205 [9]. PCC, GCC and kaolin filler slurries, as received from the suppliers, were directly added to the pulp to achieve desired filler ratios without retention aids. Bulk filler retentions in the handsheets were determined by a posterior 900°C ash test [10]. Handsheet identification, filler type and ash content are listed in Table 1. In order to achieve a significantly different amount of PCC at the top surface of materials P1 and P2, a higher bulk filled/pulp fiber ratio was required than in the other two cases. Introduction of retention aids might have alleviated this problem, but were not used in this study. Each set of handsheets contained 10 individual sheets. The sheets were pressed using a hydro-presser at a constant pressure of 344 kPa for

Table 1.
Sample ID, filler type and ash content for each sample

Sample ID	Filler	Ash content (%)
N	No filler	N/A
P1	PCC	14.6
P2	PCC	36.0
G1	GCC	17.7
G2	GCC	25.6
K1	Kaolin	15.6
K2	Kaolin	24.9

two cycles, one for 5 min and another for 2 min and ring-dried at 23°C and 50% RH for 24 h.

2.4. Surface Characterization

Surface morphologies of the handsheets were investigated using environmental SEM (EVO 40, Zeiss, Oberkochen, Germany). From a randomly-selected sheet for each set, a circular specimen, with an area of about 2 mm^2, was punched and mounted on an SEM stud with the top surface of the handsheet facing up, using a conductive double-sided tape. Energy dispersive X-ray (EDX) analysis was performed (Noran microanalysis system, Thermo Fisher Scientific, Waltham, MA) to assess the filler content at the test surface of each handsheet. An acceleration voltage of 15 keV and a photoelectron take-off angle of 29.46° relative to the paper surface were used. Data were acquired over an area of 0.064 mm × 0.086 mm under magnification 50× and working distance of 15 mm. As the chemical compositions of the fillers were distinct from the paper, EDX was used to detect filler concentrations near the surface. Calcium Ca (20) was exclusive to calcium carbonate fillers and aluminum A1 (13) and silicon Si (14) were only present in the kaolin.

Noncontact optical profilometry was performed using a white-light interferometer (Zygo Corporation, Middlefield, CT) to characterize surface topography. Circular specimens with an area of about 2 mm^2 were punched from each sample and mounted on a glass substrate with the top surface facing the interferometer. The surface was imaged using a 10× Mirau objective with field of view (FOV) of 0.70 mm x 0.53 mm and an in-plane resolution of 1.10 μm. Ten measurements were acquired for each material and the root mean square (RMS) roughness, R_{RMS}, of the surface was calculated.

2.5. Double Cantilever Beam and Peel Specimen Preparation

A double cantilever beam (DCB) specimen, shown in Fig. 2, was used to assess the toughness of the PSA–handsheet interface. The beams of the DCB specimen were fabricated from polycarbonate: Young's modulus E = 2.2 GPa. Each beam had length L = 60 mm, width b = 10 mm and thickness h = 2.38 mm. The PSA

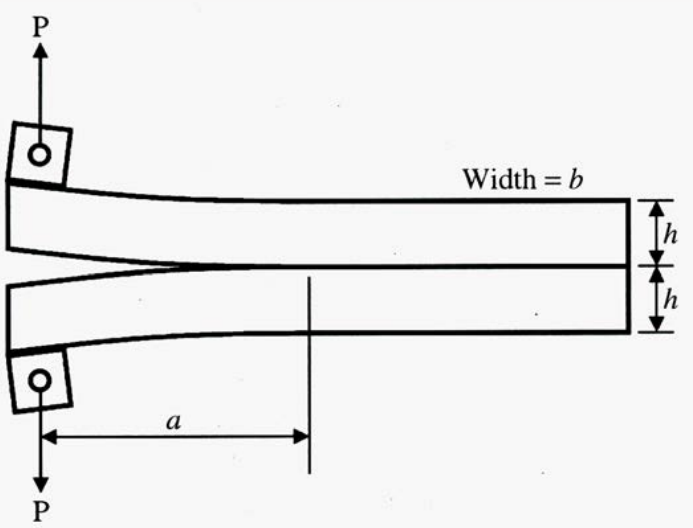

Figure 2. Schematic of DCB specimen.

label-handsheet laminate was 15 mm long and 10 mm wide, the latter dimension selected to match beam width, and was adhered to the polycarbonate beams with a double-sided tape (3M 9500 adhesive transfer tape). The laminate was adhered at the end of the specimen opposite the loading studs, thus resulting in an initial crack length of 45 mm. The top and bottom beams as well as the laminate were aligned in a custom alignment fixture and then a pressure of 21.8 kPa was applied for 45 min to ensure good bonding. Finally, loading studs with nominal dimensions of 4.76 × 4.76 × 10 mm and centered through holes with a diameter of 2.5 mm were glued to the polycarbonate beams using a cyanoacrylate adhesive. For the laminates in the DCB work, the center portion of the handsheet was used and two specimens were taken from each handsheet.

Peel specimens were modified from the typical release and adhesion specimens [11] in the following ways. Physical dimensions of the PSA labels were 25 mm wide and 67 mm long. The PSA label was adhered to the handsheet top surface except for 5 mm of the 67 mm length, which was used for a grip attachment region. The initial peel front is located on the handsheet, such that as the label is peeled, the peel front does not cross over a cut edge of the handsheet in order to minimize the likelihood of paper failure [8]. The laminate was rolled with a 2240 g, 63 mm wide roller along the length of the label 10 times forward and backward. Parallel cuts, 5 mm outside of each long label edge, were made, yielding a 35 mm wide specimen with a PSA label centered along its width. This laminate was attached to the steel translating sled with a double-sided tape. An auxiliary paper strip was adhered to the 5 mm label tab and inserted into the test machine grip. Peel length was approximately 62 mm. Eight replicates were performed for each sample.

2.6. Peel Strength Measurements

A TMI Lab Master Release and Adhesion System (Testing Machines Inc, New Castle, DE) was used for all peel tests. All tests were performed with the sled oriented at

90° and the PSA label was peeled from the handsheet. Sled speed was 305 mm/min. Tests were performed in an environmentally-controlled room at 23°C, 50% RH.

2.7. Double Cantilever Beam Toughness Measurements

The strain energy release rate, G, for the DCB specimen is calculated by considering the change in strain energy in the specimen as the crack advances [12]:

$$G = \frac{12P^2a^2}{b^2h^3E}, \tag{1}$$

where P is applied load, b is specimen width, h is beam thickness, a is crack length and E is Young's modulus of the beam material. At failure the critical strain energy release rate is calculated from equation (1) based on the crack length and applied load.

Specimens were tested on an Instron electromechanical test machine (Model 5865) in displacement control at a constant crosshead speed of 1.0 mm/min. Tests were performed in an environmentally-controlled room at 23°C, 50% RH. A high-resolution CCD camera was used to monitor the crack initiation and crack propagation and used to verify failure at the PSA–handsheet interface.

3. Results and Discussion

3.1. Characterization of Filler Particles

The size distribution of particles for each filler is shown in Fig. 1, while the morphologies of individual filler particles in the handsheets as examined by SEM are shown in Fig. 3. For PCC, the SEM image in Fig. 3 shows an aggregate particle; the smaller features of the individual particles are evident. The aggregation occurs during handsheet forming, so direct comparison of data from Figs 1 and 3 was not possible for PCC. The particle sizes in Figs 1 and 3 are in reasonable agreement for GCC and kaolin. The size distributions are similar for PCC and kaolin, both have a narrow ranges of sizes, while GCC has a broader range of particle sizes. The SEM images in Fig. 3 verified the geometries of the fillers as specified by the suppliers, namely, rhombic PCC, hexagonal kaolin and amorphous GCC.

3.2. SEM and EDX Analyses of Filler Content at the Paper Surface

Examination of the handsheet top surfaces by SEM (Fig. 4) shows the network-like structure of paper with fiber–fiber bonds and crossings as well as the sparsely distributed filler particles. Some filler particles are located on the top surface of the fibers, whereas others appear in voids. Filler particles situated between fibers within the inter-fiber bonding regions are not visible. Filler particles in these inter-fiber bonding areas are expected to reduce the internal bond strength of the paper [13]. In contrast, these particles within surface voids do not influence inter-fiber bonds. These SEM images are used to assess how bulk filler loading affects the number and

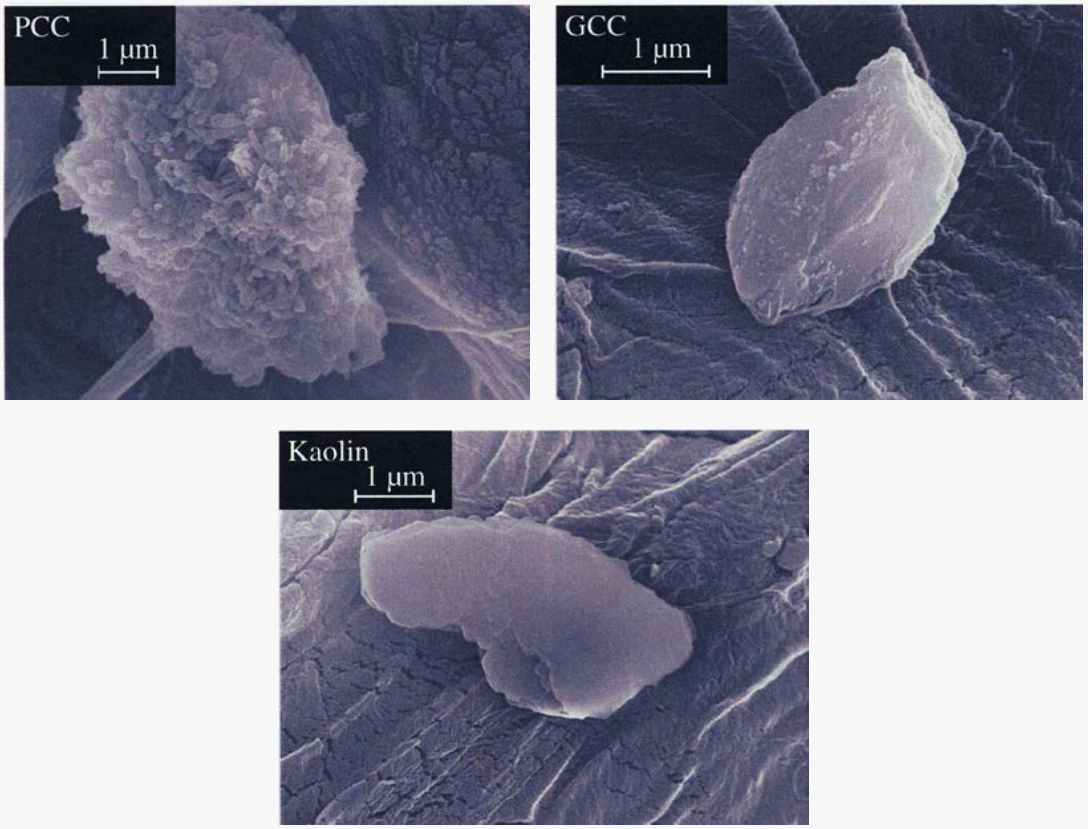

Figure 3. High magnification SEM images of three types of filler particles in handsheets: PCC, GCC and kaolin.

distribution of filler particles on the surface and to determine the effectiveness of the sample preparation procedure. SEM images of PCC and GCC handsheets with high filler levels, designated P2 and G2, showed more filler particles on the surface than corresponding handsheets with low filler levels, P1 and G1. A similar conclusion is not possible for kaolin images, K1 and K2. The images shown in Fig. 4 for each type of handsheet are representative of multiple SEM observations that were made on different samples taken from the handsheets.

An EDX analysis, which quantitatively measures the specific elements present near the surface, was also used to compare the amount of filler near the top surface of the handsheet for the two filler concentrations. The EDX spectra for the six handsheet types are shown in Fig. 5; note the different ordinate scales in the six plots. Spectral intensities for PCC and GCC were in good agreement with observations made by SEM. Specifically, the EDX measurements suggest a much higher concentration of filler near the surface in the samples with higher bulk filler concentrations. For the kaolin, the spectral intensity of K2 was only slightly higher than that of K1. While ash test results indicated 66% more filler in K2 as compared to K1, EDX results showed only moderately more filler at the top surface of those handsheets.

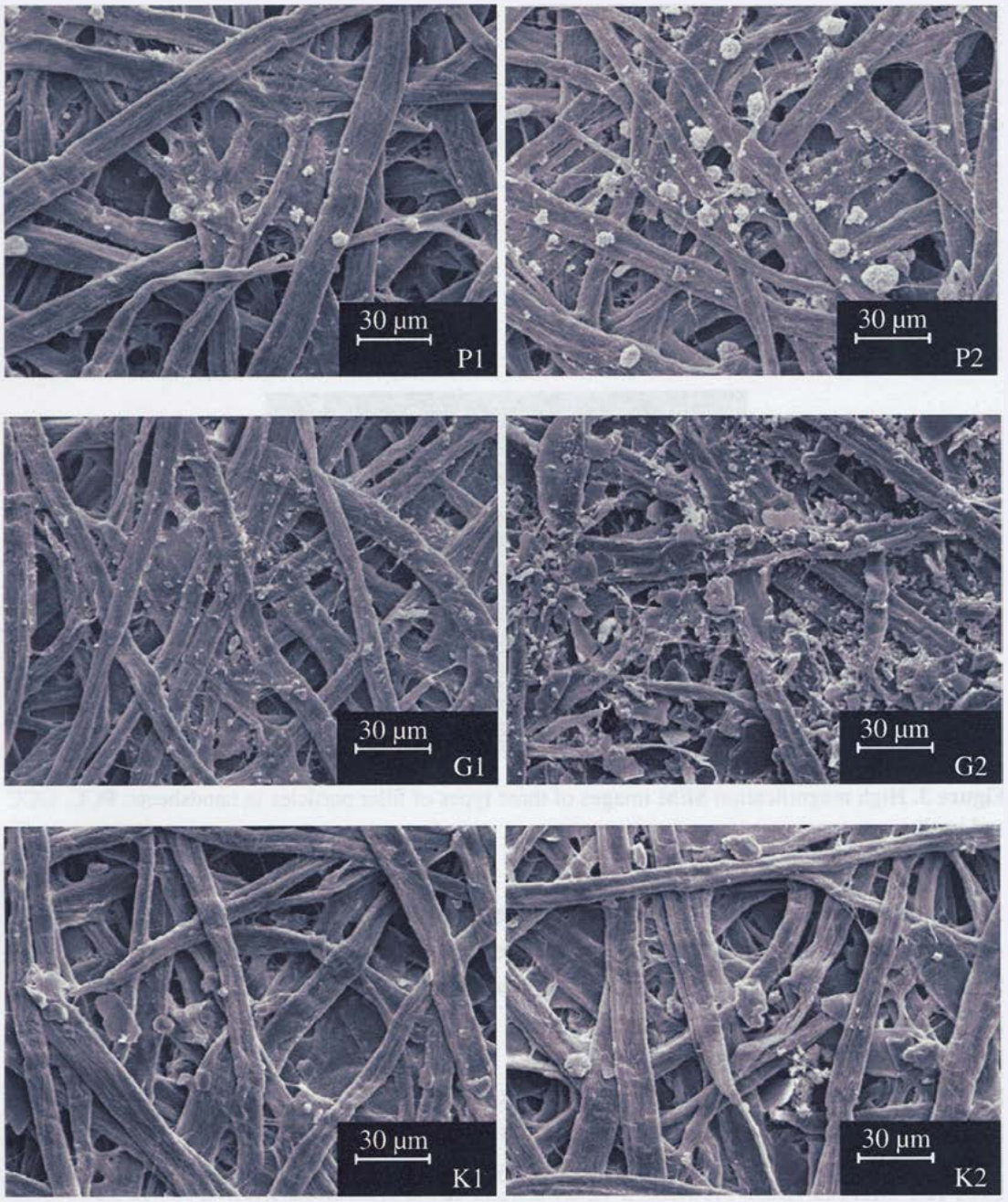

Figure 4. SEM images of handsheet surfaces for P1 with 15% PCC; P2 with 35% PCC; G1 with 15% GCC; G2 with 25% GCC; K1 with 15% kaolin and K2 with 25% kaolin.

3.3. Topography Measurements of Paper Surfaces

As seen from the SEM images (Fig. 4), the filler particles on the surface of the paper are sparsely distributed and are small compared to the size of the fibers. As such, the particles are not expected to have a significant effect on the topography of the paper. Indeed, interferometry measurements of a control handsheet with no filler and a handsheet with 25% GCC (Fig. 6) show that the natural network structure

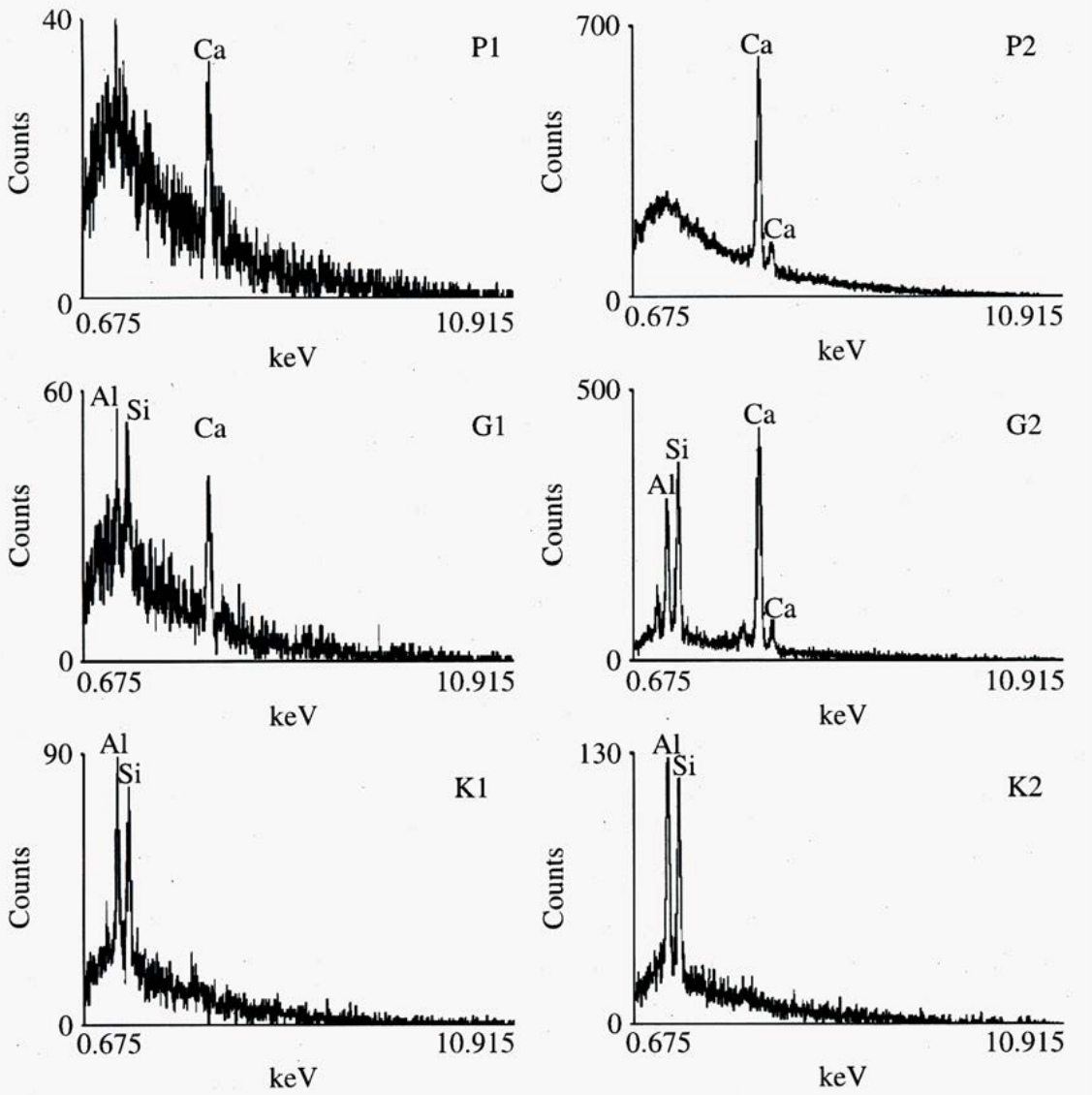

Figure 5. EDX spectra of handsheet surfaces for P1 with 15% PCC; P2 with 35% PCC; G1 with 15% GCC; G2 with 25% GCC; K1 with 15% kaolin and K2 with 25% kaolin. Note the different scales on the ordinate axes.

of the paper dominates the topography and that the filler has only little effect. The root mean square roughness, R_{RMS}, values of all the samples are summarized in Fig. 7(a) and indicate that there is no significant difference in the surface roughness among any of the handsheet samples investigated. Figure 7(b) shows the average power spectral density as a function of spatial frequency for all the samples. The power spectral density provides a measure of the height of features on the surface as a function of spatial frequency. In Fig. 7(b), no difference is observed among the samples at low spatial frequencies (long wavelengths) and only small differences are observed at higher frequencies. At high spatial frequencies, all of the samples except G1, P1 and P2 have a similar power spectral density to the handsheet without

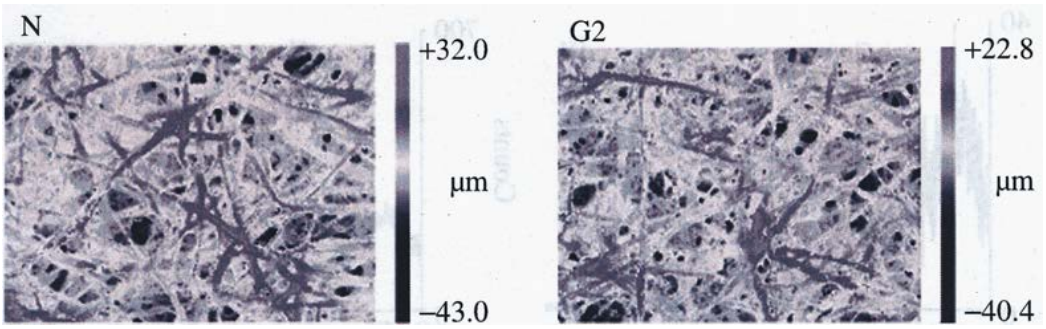

Figure 6. White-light interferometry measurements of the topography of handsheet top surfaces with no filler (left) and 25% GCC (right). Each image measurement covers an area of 0.70 mm x 0.53 mm.

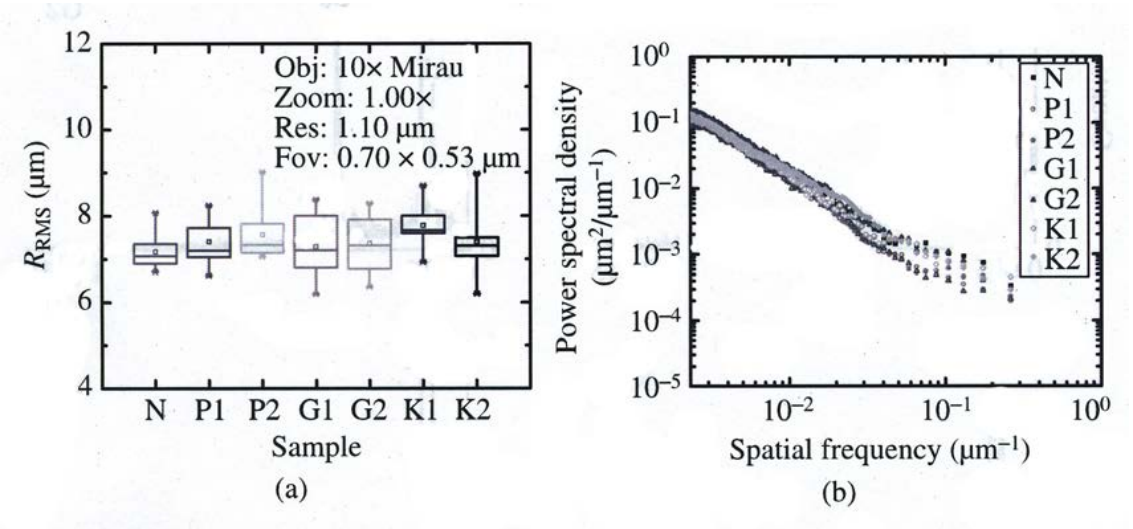

Figure 7. Comparison of the surface topography of hte seven handsheet samples. All measurements based on white-light interferometry measurements of the top surface of handsheets. (a) RMS roughness of each sample, 10 individual measurements for each sample. (b) Power spectral density for the seven handsheet samples.

filler. The results indicate that G1, P1 and P2 have slightly lower amplitude than the control at higher frequencies, but the difference is small.

3.4. Peel Measurements

The typical peel curves for N and G2 samples are shown in fig. 8. In all the tests, the peeling occurs at an approximately constant load with only minor fluctuations over the full travel distance of the sled. Figure 9 summarizes the results from the peel tests; each sample had eight replicates. The peel strength for each individual test is defined as the average peel force measured over 20 mm to 60 mm of sled travel.

Overall, the filled handsheets have higher peel strengths than the non-filled handsheet (N). The peel strengths of PCC and GCC handsheets decrease with increased filler loading level, while the kaolin handsheets show no difference in peel strength with filler loading level. The decrease in peel strength with higher loading in the

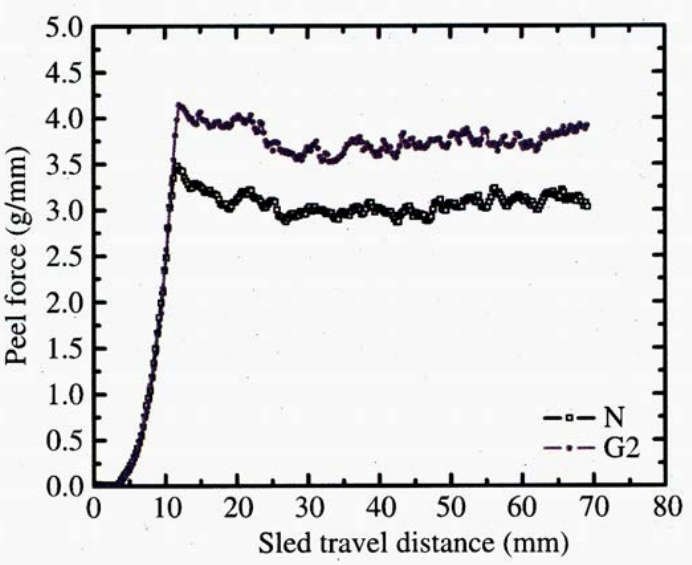

Figure 8. Examples of typical force-distance curves in the peel tests. Results are shown for one specimen each from N and G2.

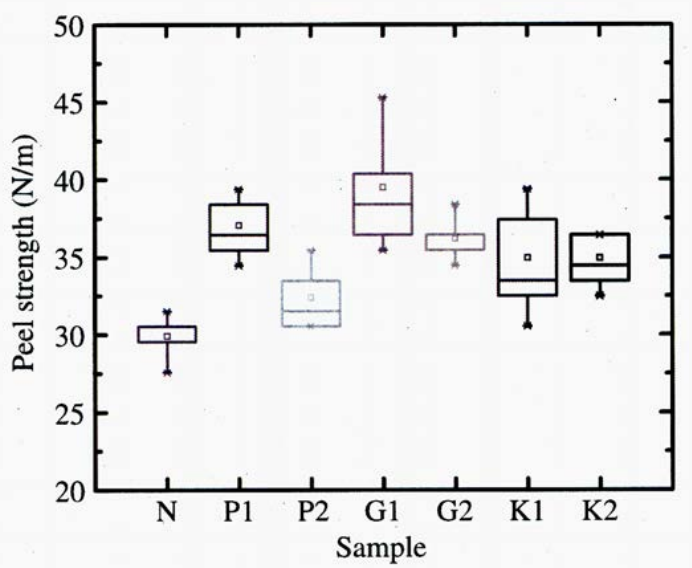

Figure 9. 90° peel strength for each sample. For each sample, there are 10 individual measurements.

PCC and GCC is likely due to a loss of internal paper strength with the addition of more filler. The surface of the PSA after peeling (Fig. 10) clearly indicates a mixed failure mode that occurs through a combination of paper failure, indicated by observation of fiber pull-out, and interfacial failure between the PSA and handsheet, suggested by the fact that there are regions where no fibers are observed on the PSA after peeling. The peel curves (Fig. 8) show a small drop in peel force after initiation which also suggests partial paper failure. Previous work [6] has shown that a drop in peel force after initiation indicates paper rather than interface failure; the drop in peel force observed in the present work is much less drastic than that reported in

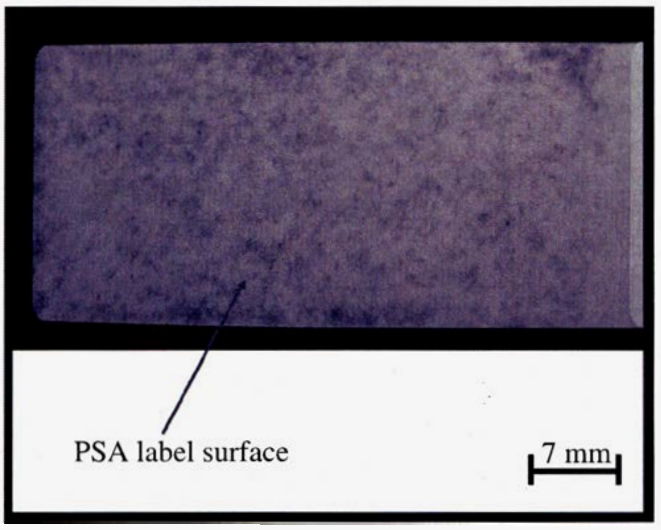

Figure 10. Photograph of PSA label surface after 90° peel test. The dark gray areas are fibers that were pulled out from the handsheet during peeling.

[6]. However, it is reasonable that the magnitude of the drop is significantly less as the failure in the present work is mixed and includes interfacial and paper failures.

Given that the peel tests have a mixed failure mode, the loss of internal paper strength would be expected to result in a decrease in peel strength. Higher levels of fillers have previously been shown to reduce the internal paper strength [2, 3] as well as peel strength [13]. The fact that the same decrease in strength with increasing filler loading does not occur for the kaolin samples may be due to surface filler concentrations that are different than bulk as well as the fact that kaolin is known to have a smaller effect on paper strength than PCC or GCC. As discussed previously, the SEM images (Fig. 4) and the EDX spectra (Fig. 5) for the two kaolin handsheets suggest that the difference in concentrations of filler near the surface of handsheets with different loadings is relatively small, which is consistent with the absence of a difference in the peel strengths. Also, previous work [14] (as cited in [13]) has shown that paper filled with clay shows a smaller reduction in bulk strength as compared to papers filled with PCC and GCC.

The results from the peel tests clearly suggest that the addition of fillers can improve the paper-PS A adhesion as indicated by the statistically significant difference in the peel strengths between the filled sheets and the unfilled sheet. However, the extent of improvement cannot be fully determined by the peel test as failure of the paper occurs. Thus, from the peel results alone, it is unclear if higher filler contents positively or negatively affect PS A-paper adhesion.

3.5. Double Cantilever Beam Measurements

Typical force–displacement curves from the DCB tests are shown in Fig. 11. The force increases initially and then drops during crack propagation. Figure 12 summarizes the critical strain energy release rates as determined from the DCB tests. There were five replicates for each sample. We note that the use of equation (1) to

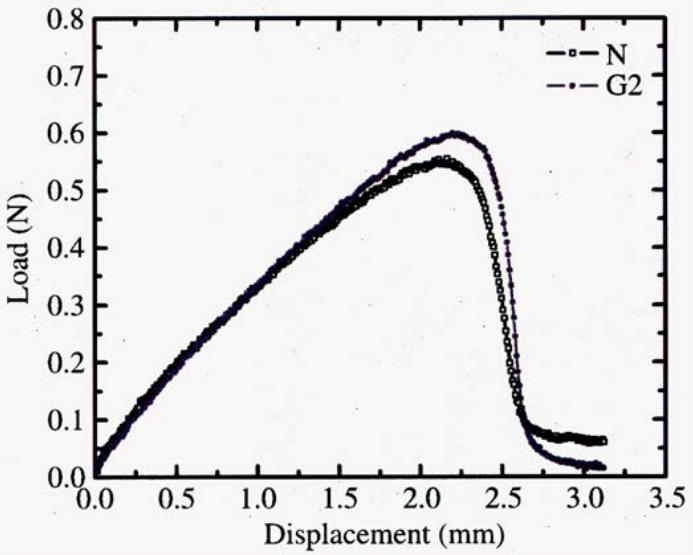

Figure 11. Examples of typical force-distance curves in the DCB tests. Results are shown for one specimen each from N and G2.

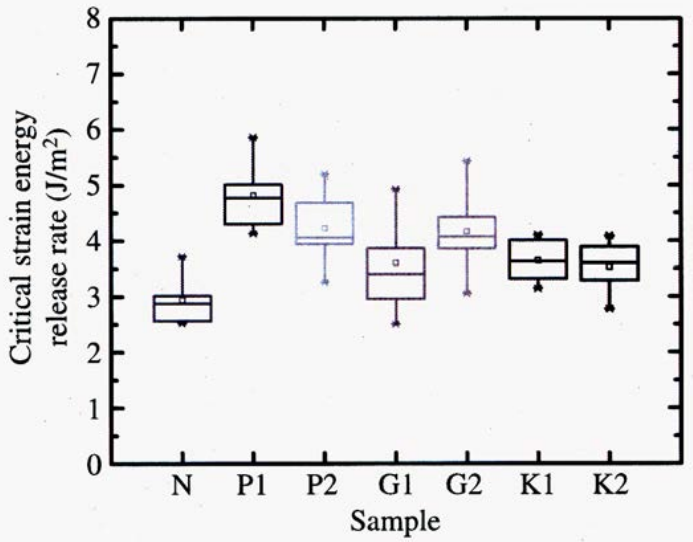

Figure 12. Critical strain energy release rates measured in DCB tests. There were 5 replicates for each sample.

calculate the strain energy release rate for the current specimen is an approximation as the equation only accounts for elastic bending energy in the beam and does not include elastic deformation that occurs in the laminate at the interface. However, this limitation should not affect the ability to make comparisons among the different samples in the current work as all samples use a laminate with the same adhesive and have a similar overall elastic response.

The fracture surface of a typical DCB specimen after testing is shown in Fig. 13 and had no visible transfer of dyed fibers to the PSA label. This is in contrast to

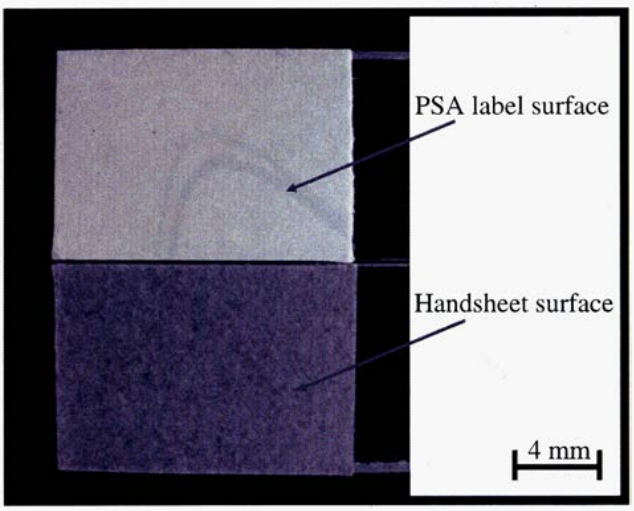

Figure 13. Optical micrograph of a post-failure DCB specimen showing pure interfacial failure.

the peel test fracture surface (Fig. 10) that showed significant fiber transfer. This suggests that the DCB measurements may provide a more representative measure of the adhesion property of the PSA–paper interface as the failure appears to be interfacial. The surface of the PSA after fracture testing was examined using optical microscopy (magnification ranging from 100 to 1000×) to assess if filler particles had been pulled from the paper surface. Across all samples, there was no evidence of transfer of filler particles to the PSA, suggesting failure occurred through a combination of failures at the PSA–cellulose fibers and PSA–filler interfaces.

There are two factors that contribute to the difference in failure modes between the peel and DCB tests. First, adhesive deformation rates in the peel test are considerably higher than in the DCB tests (305 mm/min in peel *versus* ~0.25 mm/min in DCB). As PSAs exhibit a strong viscoelatsic response, the strength of the PSA is expected to be considerably higher in the peel experiments. Previous work in which PSAs were peeled from paper showed a greater instance of paper failure as peel rate was increased [8]. The other factor that may contribute to the differences in failure mode between the peel and DCB specimens is the deformation and loading induced near the crack tip during the tests. In the 90° peel test, significant out-of-plane deformation occurs at the blunt peel front which may encourage fiber pull-out and paper delamination. Conversely, the DCB specimen largely constrains the out-of-plane deformation of paper because of the stiff polycarbonate cantilever beams that support the paper and label. This constraint may encourage interfacial failure and help to minimize surface failure of the paper.

The critical strain energy release rates (Fig. 12) have an overall trend similar to the peel strengths (Fig. 9). The critical strain energy release rates of the filled handsheets are clearly higher than the sample without filler. This indicates that surface fillers are helpful in increasing PSA–paper interfacial strength. The higher adhesion strength for filled papers may be a result of greater contact area between the PSA and paper as well as an increase in surface energy due to the presence of

the fillers. Comparison of papers with the same filler and different concentrations shows an increase in critical strain energy release rate with increasing filler content for GCC and that critical strain energy release rate is independent of filler concentration for the PCC and kaolin samples. From the SEM images and EDX spectra in Figs 4 and 5, the GCC samples with higher filler loading are observed to have a greater number of filler particles at the surface. This result, in contrast to the peel tests which were limited by the internal strength of the paper, illustrates that fillers can increase PSA–paper adhesion. There is no statistical difference in the critical strain energy release rates between the high and low filler concentrations for PCC and kaolin sheets. The kaolin result is consistent with the peel results and indicates that over the range examined the filler content has only little effect on PSA–paper adhesion. Similarly, the PCC results indicate only little effect of filler content on interfacial strength at the filler concentrations investigated.

4. Summary and Conclusions

Overall, the adhesion between the PSAs and handsheets examined in this work is quite high and none of the cases has a sufficiently low strength that would prohibit their use for many applications. While the strength of all of the interfaces is adequate, the present results illustrate the multiple ways in which fillers can affect PSA–paper adhesion strength. The addition of inorganic fillers to paper has a positive effect on the adhesion of pressure-sensitive adhesives as indicated by a general increase in adhesion strength for filled papers compared to unfilled paper. However, fillers can also reduce the internal strength of paper, thus the benefit of adding filler is limited if the PSA is peeled from the paper in a manner that allows failure *via* paper delamination. The DCB specimen can characterize the actual interfacial critical strain energy release rate of PSA–paper bond as it allows the PSA to be delaminated from the paper without fiber pull-out or interlaminar failure of the paper. When failure is isolated to the PSA–paper interface, improvements in adhesion can be achieved by adding GCC at higher loading levels. However, PCC and kaolin show no distinct trend with filler concentration.

Acknowledgements

This work was supported by US Forest Service, Forest Products Laboratory and United States Postal Service. The authors thank T. A. Kuster at the Forest Products Laboratory and R. K. Noll at the Materials Science Center of UW-Madison for help with SEM and EDX. Finally, the support of Imerys and Mississippi Lime, who provided the inorganic fillers, is greatly appreciated.

References

1. R. W. Hagemeyer (Ed.), *Pigments for Paper*. TAPPI Press, Atlanta, GA (1984).
2. G. H. Fairchild, *Tappi J.* **75** (8), 85–90 (1992).

3. N. Al-Mehbad, *Polym.-Plast. Technol. Eng.* **43**, 963–979 (2004).
4. D. Satas (Ed.), *Handbook of Pressure Sensitive Adhesive Technology*. Satas & Associates, Warwick, RI (1999).
5. B. Zhao and R. Pelton, *Tappi J.* **3** (7), 3 (2004).
6. B. Zhao and R. Pelton, *J. Pulp Paper Sci.* **31**, 33–38 (2005).
7. B. X. Zhao, L. Anderson, A. Banks and R. Pelton, *J. Adhesion Sci. Technol.* **18**, 1625–1641 (2004).
8. R. Pelton, W. Chen, H. Li and M. R. Engel, *J. Adhesion* **77**, 285–308 (2001).
9. TAPPI Test Method T205 sp-02, *Forming Handsheets for Physical Tests of Pulps* (2002).
10. ISO 2144:97, *Paper, Board and Pulps — Determination of Residue (Ash) on Ignition at 900° C* (1997).
11. ASTM D6862-04, *Standard Test Method for 90 Degree Peel Resistance of Adhesives* (2004).
12. T. L. Anderson, *Fracture Mechanics: Fundamentals and Applications*. CRC Press, Boca Raton, FL (2004).
13. L. Li, A. Collis and R. Pelton, *J. Pulp Paper Sci.* **28**, 267–273 (2002).
14. H. P. K. Beazley, *Wochenblatt Papierfabrik* **103**, 143–147 (1975).